TR-2H4R
22 January 1962
Copy 87

US

ARMY ORDNANCE MISSILE COMMAND

A GENERAL PROBE THEORY FOR MEASUREMENTS IN A PLASMA

Ordnance Management Structure Code No. 5210.11.140
5210.11.148
5210.12.132

Department of the Army Project No. 503-03-009
516-01-006
516-04-007

DESTRUCTION

This report shall be destroyed when no longer required.

22 January 1962 TR 2H4R

A GENERAL PROBE THEORY FOR MEASUREMENTS IN A PLASMA

By

Charles M. Cason and T. A. Barr, Jr.

PLASMA PHYSICS BRANCH

Ordnance Management Structure Code No. 5210.11.140
5210.11.148
5210.12.132

Department of Army Project No. 503-03-009
516-01-006
516-04-007

RESEARCH LABORATORY

Research and Development Directorate

U. S. Army Ordnance Missile Command

(U) ABSTRACT

The standard model of floating probes in plasmas is reviewed. It is shown that a maximum charge density exists for the application of this model. An explicit expression of voltage applied to the probes in terms of circuit current is obtained. When certain simplifying assumptions are used, this equation is reduced to the Langmuir single probe equation and the Johnson-Malter double probe equation.

From measurements of probe current versus applied probe voltage, electron temperature at each respective probe can be determined. One example is given to illustrate the calculation.

(This abstract is UNCLASSIFIED)

TABLE OF CONTENTS

LIST OF ILLUSTRATIONS

INTRODUCTION

The analysis of gas discharge processes embodies a wide variety of theoretical explanations for a host of experimental measurements. However, present day knowledge of gas discharge properties depends primarily upon experimental measurements. Perhaps the most important variables describing a gas discharge are the electron and ion densities, and their velocity distribution functions. Meaningful measurements of temperature of plasma constituents require them to be in thermal equilibrium. When this condition is satisfied, knowledge of electron and ion properties as determined by probes is required to calculate important plasma properties such as ambipolar diffusion coefficients, excitation rates, and ionization rates. There are at present various methods for analyzing probe data which are valid for special experimental sets of conditions. Workers in this area of plasma analysis occasionally invalidate their results by using a theory in experimental situations where the assumptions are inapplicable. It is the purpose of this paper to show the connection of these various probe theories, and to produce a generalized theory. A simple derivation of probe theory is presented which holds for various probe area ratios; the probes are not required to be surrounded by identical plasmas.

THEORY

GENERAL PROBE THEORY

Standard treatment of experimental data taken by probe methods allows the assumption of flat plate geometry according to a proof by Druyvesten (ref. 1), who concluded that any convex shape for a probe should be appropriate. The plasma sheath condition requires, according to Langmuir in reference 2, that only a few percent of electrons falling on the sheath may collide with sheath constituents before being collected by the probe. Hard sphere collisions of electrons with neutral particles are assumed to dominate any effect of scattering interactions between charged particles within the plasma. The limitations on this latter assumption will be discussed in appendix A. A Maxwell-Boltzmann distribution of particle speeds is assumed so that the concept of temperature may be used. Probes are considered cold, and consequently do not emit electrons.

The rate of sampling charged particles by the probes is assumed to be small compared to the rate of charge generation of the local plasma, so that the plasma's properties outside the probe sheath will not be modified. If the plasma is generated from thermal excitation in a dense gas, the conditions required for this assumption are possible to obtain. The primary condition required of the plasma, (discussed in more detail in appendix A), is that the plasma be diluted by neutral gas atoms in thermal equilibrium. The plasma, consisting only of positive ions of the gas species and free electrons, constitutes a very small percentage of the total number of particles present.

The basic equations governing the potentials on each of the two probes in this model are determined from Kirchhoff's law. As shown in figure 1, the ion currents to the probes are $i_i \times A$ where i_i is the random ion current in the plasma around the probe and A is the probe area. A similar notation for random electron current is used, in which i_e is the random electron current. Conventional current in the external circuit is denoted by I. Primed notations are used to refer to the part of the total random currents which are collected by a probe as determined by the probe's potential, while subscripts refer to probe 1 and 2. Figure 1 shows from Kirchhoff's law that

$$i'_{i1}A_1 - A_1 i'_{e1} + I = 0, \tag{1}$$

and

$$i'_{i2}A_2 - A_2 i'_{e2} - I = 0, \tag{2}$$

where A_1 and A_2 are the areas of the two probes. Note that only one primed term per equation is allowed since $i_i' = \int_V^{\infty} f(v)dv$ and $i_e' = \int_{-\infty}^{-V} f(v)dv$ and each probe must be at a single potential. The function f(v) is the distribution function for x component of velocity, where $V = mv^2(1/2\epsilon)$, m and ϵ are the electron mass and charge, and v is the velocity of the electron.

The solutions for this integration, when a Maxwellian distribution function is assumed are

$$i_e' = \frac{m}{4}\epsilon\left(\frac{8}{\pi}\frac{kT_e}{m}\right)^{1/2} \exp(+\epsilon V/kT_e) \tag{3}$$

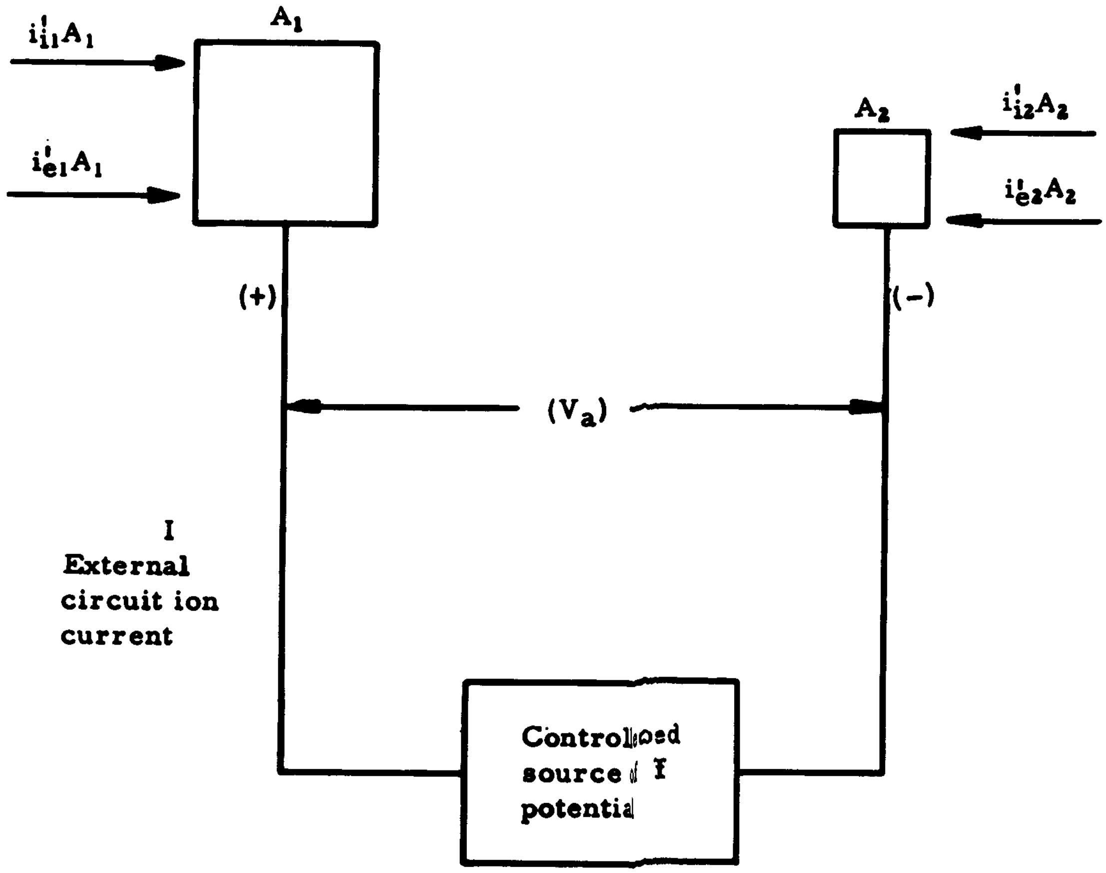

Probe A is assumed to be more negative than probe 1

Figure 1. - Schematic diagram of probe circuit.

and

$$i_i^{\prime} = \frac{M}{4}\epsilon\left(\frac{8}{\pi}\,\frac{kT_i}{M}\right)^{1/2} \exp\left(-\epsilon V/kT_i\right) \tag{4}$$

where M is the ion mass, T the temperature in degrees Kelvin and k is the Boltzmann constant. Equation (3) may be substituted into (1) and (2), where both probes are assumed to be at negative potentials with respect to the plasma to give the negative potential equations:

$$V_1 = T_{e1}(k/\epsilon)\ \ln\left[(1 + I/i_{i1}A_i)(i_{i1}/i_{e1})\right], \tag{5}$$

and

$$V_2 = T_{e2}(k/\epsilon)\ \ln\left[(1 - I/i_{i2}A_2)(i_{i2}/i_{e2})\right]. \tag{6}$$

The random electron current terms are a convenient grouping of constants from the integration. By setting I equal to zero, the floating potential V_f for any surface is found to be

$$V_f = \tfrac{1}{2}T_e(k/\epsilon)\ \ln\left(\frac{mT_i}{MT_e}\right), \tag{7}$$

which is in its standard form, assuming thermal equilibrium. This potential is negative with respect to the plasma potential when $|i_e| > |i_i|$ which is true for most cases.

Companion equations to (5) and (6) are developed when the probes are assumed to be at some positive potential with respect to the floating plasma potential. Equation (4) is substituted in (1) and (2) to give the positive potential equations

$$V_1 = -\,T_{i1}(k/\epsilon)\ \ln\left[\left(\frac{1 - I}{i_{e1}A_1}\right)\left(\frac{i_{e1}}{i_{i1}}\right)\right], \tag{8}$$

and

$$V_2 = -\,T_{e2}(k/\epsilon)\ \ln\left[\left(\frac{1 + I}{i_{e2}A_2}\right)\left(\frac{i_{e2}}{i_{i2}}\right)\right]. \tag{9}$$

Here, the random ion current terms represent a convenient grouping of constants from the integration. The positive and negative potential equations may be added to yield complete expressions for probe potentials. Measurements of circuit voltage represented by V_a in figure 1,

correspond in an experiment to differences of probe potential, as illustrated in figure 2. Differences between the complete expressions for probe potentials, taken as indicated in figure 2, will yield the explicit equation of V_a for the current-voltage probe characteristic:

$$V_a = T_{i1}(k/\epsilon)\ \ln\left[\left(\frac{1 - I}{i_{e1}A_1}\right)\left(\frac{i_{e1}}{i_{i1}}\right)\right] - T_{i2}(k/\epsilon)\ \ln\left[\left(\frac{1 + I}{i_{e2}A_2}\right)\left(\frac{i_{e2}}{i_{i2}}\right)\right] + T_{e2}(k/\epsilon)\ \ln\left[\left(\frac{1 - I}{i_{e2}A_2}\right)\left(\frac{i_{i2}}{i_{e2}}\right)\right] - T_{e1}(k/\epsilon)\ \ln\left[\left(\frac{1 + I}{i_{i1}A_1}\right)\left(\frac{i_{i1}}{i_{e1}}\right)\right] \cdot \tag{10}$$

While equation (10) holds for all values of external circuit current up to its limiting value as determined by the probe area and Kirchhoff's law,

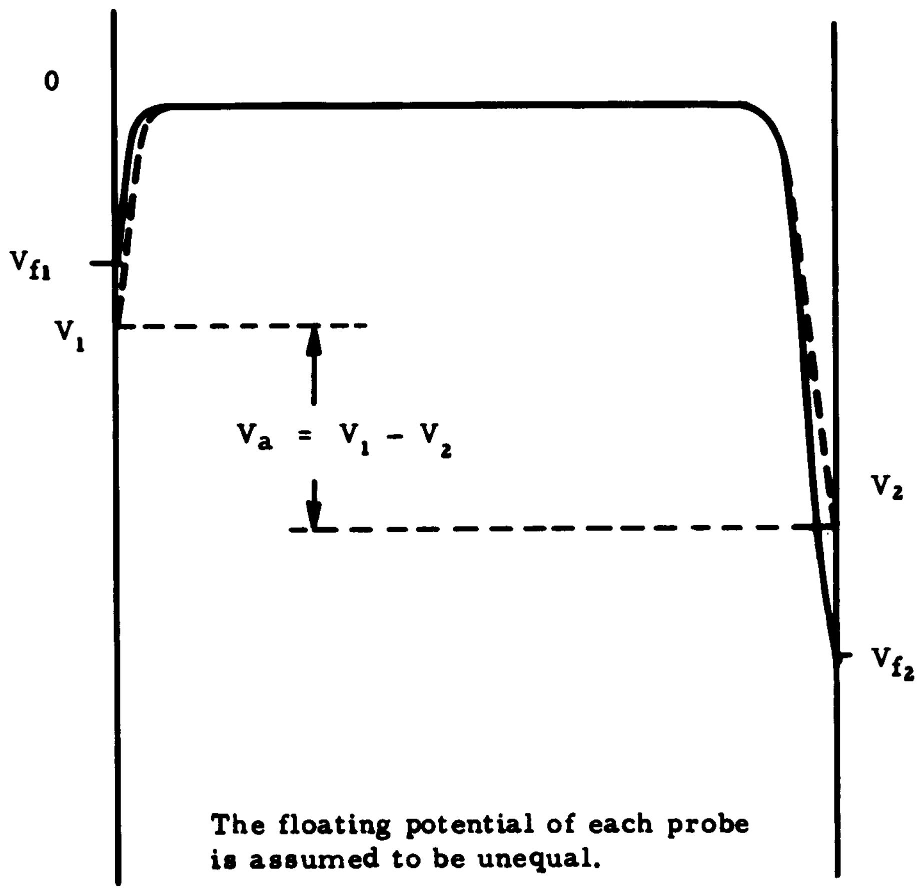

Figure 2. - Potential diagram for two probes in a plasma.

only two terms appear in the calculation at any one time. When a given probe is positive, only its contributing term with ion temperature as a coefficient appears and the other term vanishes. For a negative probe, its contributing term with the electron temperature as a coefficient appears and its other term vanishes.

MATHEMATICAL CHARACTERISTICS OF THE PROBE POTENTIAL EQUATIONS

It is important to recognize the special properties of the negative potential equations (eqs. 5 and 6). The following definitions will be used in this section to simplify analysis:

$$B_1 = \frac{I}{i_{i1} A_1} \tag{11}$$

and

$$B_2 = \frac{I}{i_{i2} A_2} \tag{12}$$

Potentials of each probe will be normalized by using the electron temperature as a unit of voltage:

$$\eta = \frac{V}{T_e} \tag{13}$$

$$\eta_a = \quad {}_2 - \eta_1 \tag{14}$$

Equations (5) and (6) may be rewritten when $T_e = T_i$ at each probe with the above definitions:

$$\eta_1 = \ln \left[(1 + B_1)(m/M)^{1/2}\right] \tag{15}$$

and

$$\eta_2 = \ln \left[(1 - gB_1)(m/M)^{1/2}\right] \tag{16}$$

where $g = B_2/B_1$

Figure 3 is a plot of η_1 and η_2 for hydrogen where the ion mass is 1.0 amu. It should be noted that η_1 is limited to each value of g determined by the maximum allowed circuit current. For values of g above about 45, the small probe is allowed to acquire positive potentials. For $g = 100$, it is seen from the figure that η_1 is limited to + 0.87 for

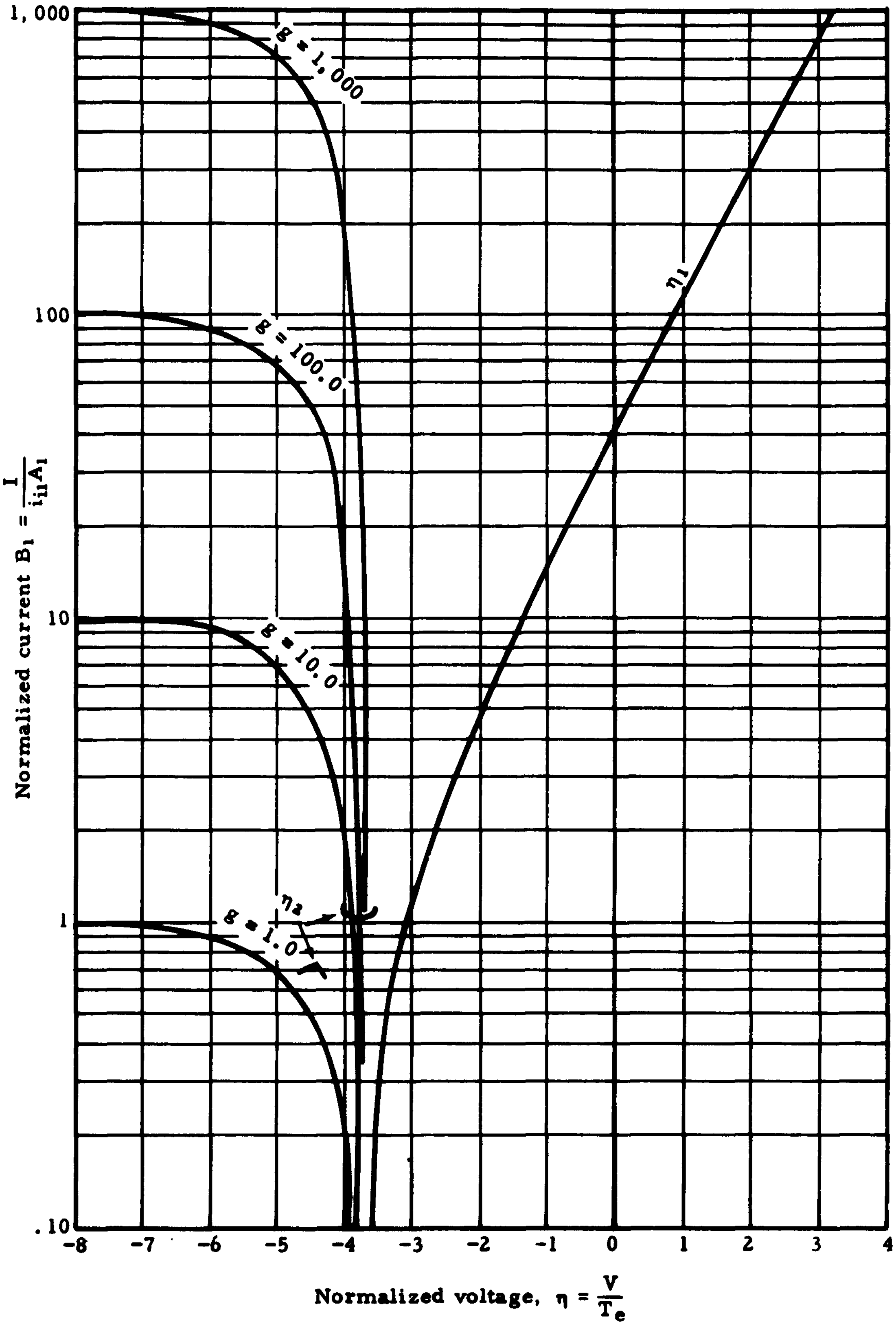

Figure 3. - Normalized current versus normalized voltage on each probe.

η_2 approaching $-\infty$. The Langmuir theory (discussed later) is valid for hydrogen only when η_2 is nearly equal to -3.76. Large area ratios are often required for a probe to develop significant positive potentials consistent with equation (23) when $T_{e1} = T_{e2}$.

It is often helpful to visualize the current versus voltage on a probe for a given species of particle (ion or electron) under ideal conditions. Figure 4 is a plot of the current variation with probe potential. Due to the large ratio of ion and electron masses, a scaling factor was introduced to illustrate each current on the same plot.

The point of intersection is the floating potential for the probe in a hypothetical plasma having $i_e = 4i_i$ (which of course, is not realistic for any known ion at the same temperature as the electrons in its

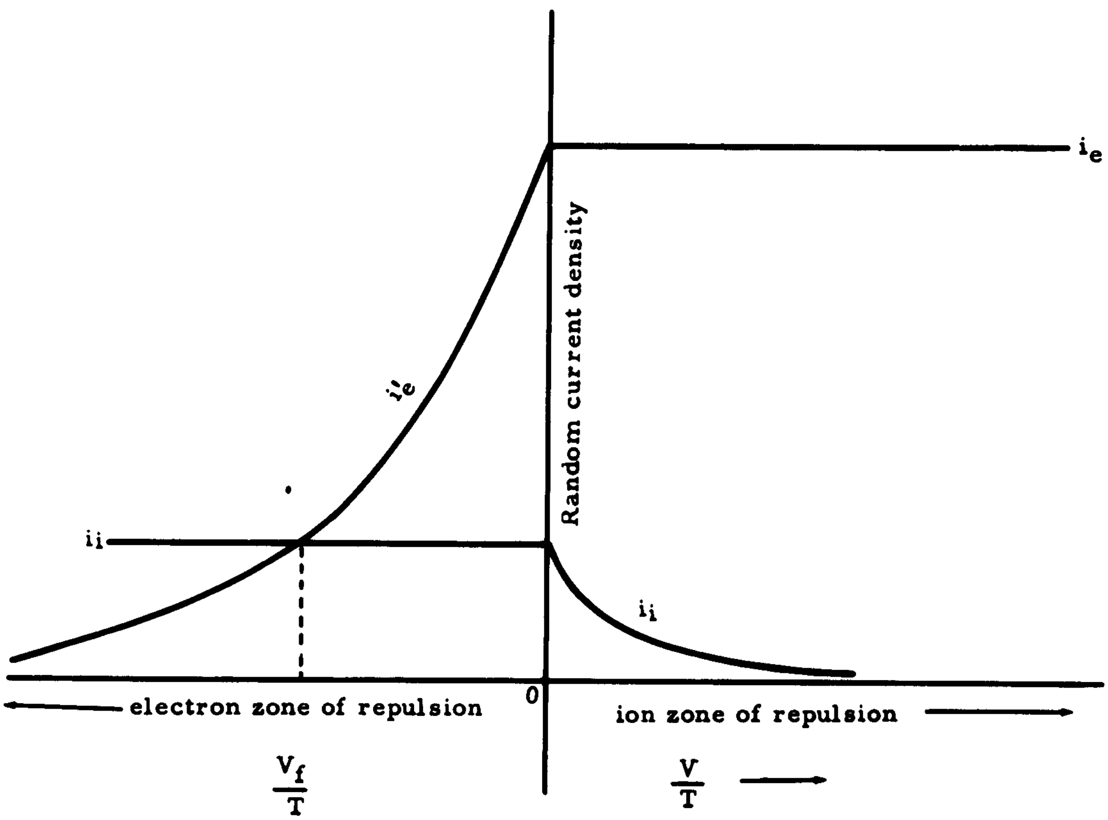

Figure 4. - Current variation with probe potential

$$(M = 16m) \qquad V_f = k/\epsilon \ln \frac{T_i m}{T_e M}^{1/2}.$$

locality.) Potential zones of attraction of particles show all random current collected by the probe of unit area. It is assumed that the sheath dimensions are fixed. Zones of repulsion between the probe and the charges show the collection current variation according to equation (3) and (4).

REDUCTION TO LANGMUIR THEORY

Consider, as an example, the behavior of equation (10) when probe 2 acquires a positive potential. The argument of the logarithm of the first and third term in equation (10) can be shown to be equal to 1 by using Kirchhoff's law, and by ascertaining terms that are fractions of the random currents. A voltmeter would then measure

$$V_a = k/\epsilon \left\{ - T_{e1} \ln \left[\left(\frac{1 - I}{i_{i1} A_1} \right) \left(\frac{i_{i1}}{i_{e1}} \right) \right] - T_{i2} \ln \left[\left(\frac{1 + I}{i_{e2} A_2} \right) \left(\frac{i_{e2}}{i_{i2}} \right) \right] \right\}, \tag{17}$$

as the external circuit voltage for external circuit current I. It is apparent that equation (17) has an operating bound. The maximum value $I_{max} = -i_{i1}A_1$ is substituted in equation (17). The required condition is that the second term must always be positive if probe 2 is to be positive, or

$$0 < T_{i2} \ln \left[\left(1 + \frac{i_{i1} A_1}{i_{e2} A_2} \right) \left(\frac{i_{e2}}{i_{i2}} \right) \right]. \tag{18}$$

The argument of the logarithm in equation (18) must therefore be less than unity. This condition establishes a requirement on both probe areas and local random ion currents for a probe to acquire a positive potential, or

$$\frac{i_{i1} A_1}{i_{e2} A_2} > \frac{i_{i2}}{i_{e2}} - 1. \tag{19}$$

If each side of equation (19) is equal, then probe 2 approaches zero potential when probe 1 approaches $-\infty$.

An important case arises when

$$\frac{i_{i1} A_1}{i_{i2} A_2} >> \frac{i_{e2}}{i_{i2}} - 1. \tag{20}$$

This is the condition for a "floating" single probe. Equation (18) is transformed into

$$V_a \approx -\tfrac{1}{2} T_{e1}(k/\epsilon) \ln\left(\frac{mT_{i1}}{MT_{e1}}\right) - T_{i2}(k/\epsilon) \ln\left[\left(\frac{1+I}{i_{e2}A_2}\right)\left(\frac{i_{e2}}{i_{i2}}\right)\right] \tag{21}$$

for the current-voltage relationship, since I is limited by $i_{e2}A_2$ which is much less than $i_{i1}A_1$.

A companion to equation (21) is developed, when the "floating" probe goes negative with respect to its surrounding plasma, by a similar treatment of equation (10) for $-$ I:

$$V_a \approx -\tfrac{1}{2}T_{e1}(k/\epsilon) \ln\left(\frac{mT_{i1}}{MT_{e1}}\right) - T_{e2}(k/\epsilon) \ln\left[\left(\frac{1-I}{i_{i2}A_2}\right)\left(\frac{i_{i2}}{i_{e2}}\right)\right] \tag{22}$$

The first term in equations (21) and (22) is recognized to be the floating probe potential for probe 1. By making use of this fact and substituting in the Kirchhoff relation for I, equations (21) and (22) may be written in a different form:

$$\begin{aligned} V_2 &= V_a + V_{f1} = T_{i2}(k/\epsilon) \ln (i_{i2}) - T_{i2}(k/\epsilon) \ln (i_{i2}^{!}) \\ V_2 &= V_a + V_{f1} = T_{e2}(k/\epsilon) \ln (i_{e2}) - T_{e2}(k/\epsilon) \ln (i_{e2}^{!}) \end{aligned} \tag{23}$$

Equations (23) were first derived by Langmuir and Mott-Smith (ref. 3) for "floating" single probes. Thus, under the approximations shown above, equation (10) may be reduced to the special case of the Langmuir single probe equation. The potential of the floating probe with respect to the surrounding plasma "zero" potential is plotted as a function of the natural logarithm of the current falling on the probe. Since the first term in each of equations (23) is a constant, the straight line slope of the current-voltage data is both a determination of the Maxwellian character of the collected charges and their temperature.

REDUCTION TO JOHNSON AND MALTER THEORY

With equation 10 as the starting point, it is assumed that both probes have area ratios which fail to satisfy the conditions prescribed by equations (19)and (20). The measured voltage between the probes would then depend primarily upon the temperature and random current of the local electrons surrounding each respective probe, as seen in equation (24).

$$V_a = -T_{e1}(k/\epsilon) \ln\left[\left(\frac{1+I}{i_{i1}A_1}\right)\left(\frac{i_{i1}}{i_{e1}}\right)\right] + T_{e2}(k/\epsilon) \ln\left[\left(\frac{1-I}{i_{i2}A_2}\right)\left(\frac{i_{i2}}{i_{e2}}\right)\right] \tag{24}$$

For convenience, the Johnson and Malter model (ref. 3) assumed the probes were so close together that no significant difference between local electron temperatures would be permitted. Equation (17) is written in its simplest form by using these conditions.

$$V_a = T_e(k/\epsilon) \ln\left(\frac{A_2 i_{i2} - I}{A_1 i_{i1} + I}\right) \tag{25}$$

Differentiation of equation (25) results in

$$\left.\frac{dV_a}{dI}\right|_{V_a = 0} = T_e(k/\epsilon) \frac{(A_1 i_{i1} + A_2 i_{i2})}{(A_2 i_{i2} - I|_{V_a = 0})(A_1 i_{i1} + I|_{V_a = 0})} = R_o, \tag{26}$$

where R_o was defined as the "equivalent resistance" of the plasma. The following substitutions are required to place equation (26) in a familiar form: $\Sigma_{ip} = A_1 i_{i1} + A_2 i_{i2}$ and $G = [A_2 i'_{e2}/\Sigma_{ip}]_{V_a = 0}$

Electron temperature may then be calculated by

$$T_e = 11,600(G - G^2)R_o\Sigma_{ip} \tag{27}$$

This result was first derived by Johnson and Malter (ref. 3) as the "equivalent resistance method". Use of equation (27) has an important restriction which is worth noting. The calculated electron temperature is some sort of effective or average value when the probes are placed in a plasma of unequal local electron temperatures. For this situation, T_e does not represent the actual value at either probe.

GENERAL DOUBLE PROBE METHOD

The expression for the current-voltage relation of equation (10) may be also used for the general case in which $T_{e1} \neq T_{e2}$ and $i_{i1}A_1 \neq i_{i2}A_2$. The equation for calculating these temperatures from current-voltage data is found by expanding equation (24) to reflect the floating potential of each probe according to equation (7):

$$V_a = T_{e2}(k/\epsilon) \ln\left(\frac{1 - I}{i_{i2}A_2}\right) - T_{e1}(k/\epsilon) \ln\left(\frac{1 + I}{i_{i1}A_1}\right) - V_{f1} + V_{f2}. \tag{28}$$

The terms $V_{f2} - V_{f1}$ are the differences in floating potentials between probes 1 and 2, and will be denoted as ΔV_f as shown in figure 5. When the external circuit current is zero, the voltage measured is the difference in floating potentials. In order to calculate T_{e1} and T_{e2} from actual data, a knowledge of i_iA for each probe is required.

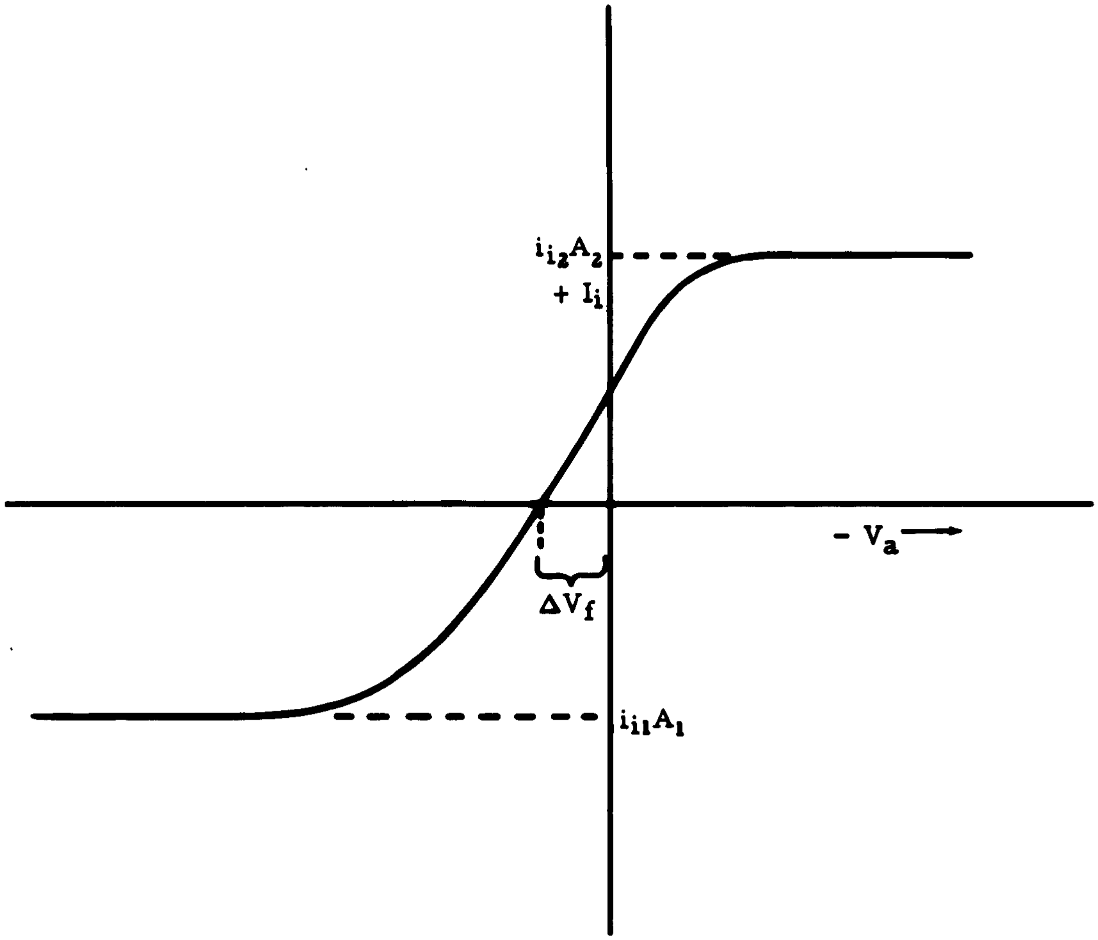

Figure 5. - Typical double probe data characteristic curve.

This quantity, i_iA, is the saturated current and should be almost constant for all values of V_a.

The following table is helpful in identifying which saturated current refers to which probe, and the appropriate signs of current-voltage for analysis of data.

An analysis of data with unequal electron temperatures is given in appendix B to illustrate the procedure.

TABLE I

TABLE OF SATURATED CURRENT IN REFERENCE TO PROBE FOR DATA ANALYSIS

Conditions	$T_{e1} > T_{e2}$	$T_{e2} > T_{e1}$
$I = 0$	V_a is positive	V_a is negative
$V_a \to +\infty$	$I \to -i_{i1}A_1$	$I \to -i_{i1}A_1$
$V_a \to -\infty$	$I \to i_{i2}A_2$	$I \to +i_{i2}A_2$
$V_a = 0$	$I = + \left\| I \right]_{V_a=0} \right\|$	$I = - \left\| I \right]_{V_a=0} \right\|$

CONCLUSION

A general probe theory has been derived which may be applied to data collected from floating probes (see eq. 10) in dilute plasmas. This theory includes the effects of the probes being placed in plasma regions of unlike temperature environments. From an explicit expression of measured voltage in terms of measured circuit current, it is shown that with appropriate simplifications the Langmuir "single probe" equation and the Johnson-Malter equation are obtained.

Appendix A

TEMPERATURE LIMITATION OF DOUBLE PROBE THEORY

A theory for determining the temperature of a plasma by electrical probes is described in the main section of this report. It is valid for electrons and ions which are scattered by neutral atoms only, since no consideration was made for Coulomb interaction between the charges. It becomes important to determine the temperature for which Coulomb forces between charges become significant in modifying the theory. Consideration of the electrical conductivity as a function of temperature will illustrate the maximum allowable temperature for which confidence may be placed in the interpretation of probe measurements by the above mentioned theory.

Calculation of electrical conductivity in a gas requires knowledge of the mobility of the charge carriers. The mobilities of charged particles in a partially ionized gas are influenced both by Coulomb and collision forces. Electrical conductivity may be easily calculated for two extreme cases, that of very little ionization and the other of almost complete ionization. The isobaric conductivities calculated for both cases, assuming thermal ionization, increase monotonically with temperature. Experimental results agree very well with the theory for each case. For the intermediate degree of ionization, there is a transition zone in which mobilities are influenced by both types of collision forces. The effluent gases from a plasma jet are of the proper temperature and density ranges to manifest conductivities characteristic of all three regions: collision, transition, and Coulomb forces.

An expression for the electrical conductivity of a gas in the low temperature region (valid to 7,000°K) was given by Lin, (ref. 4) as follows:

$$\sigma = n_e e^2 \bar{\tau} / m_e, \tag{29}$$

where σ is the gas conductivity, $\bar{\tau}$ the mean collision time for electron-atom (or molecule) collisions, and n_e, e, and m_e are the electron density (no./cm^3) the electron charge, and the electron mass, respectively. The following assumptions are implicit in the derivation of equation 29:

1. In the region considered, the gas density is large enough to provide sufficiently numerous collisions between charged particles and neutrals so that statistical equilibrium is attained;

2. No electron attachment or other long-lived interactions occur between neutral and charged particles;

3. Values of the temperature and electron density are such that the Debye shielding distance is small in comparison to any critical physical length such as probe spacing or size;

4. Electrical neutrality exists;

5. No external electric or magnetic fields exists; and

6. Due to high electron mobility relative to the ions, the electrons are the current carriers.

By appropriate evaluation of $\bar{\tau}$ from kinetic theory, equation (29) may be written for argon:

$$\sigma = 5.4 \times 10^{7} \frac{n_e}{n_t T_e^{1/2}} \text{(mho/meter)} \tag{30}$$

where n_t is the number density of neutral particles, and T_e is the electron temperature. The atomic radius of argon (given in the Handbook of Chem. and Phys.) was used in evaluating the proportionality factor, 5.4×10^7, in equation (30) and n_e is determined by Saha's ionization equation. For the case cited

$$n_e = 4.66 \times 10^{45} \frac{b'(T)}{b(T)} e^{-\frac{1.82 \times 10^5}{T}} \left(\frac{\text{electron}}{m^3}\right) \tag{31}$$

where $b'(T)$ and $b(T)$ are the partition functions for singly ionized and neutral argon, respectively, (ref. 5). By assuming the perfect gas state, the isobaric conductivity for "dilute" plasma may be determined as a function of temperature. Figure A-1 shows graphically the results of such a calculation for the 1 cm Hg isobar in an argon plasma.

For fully ionized or "dense" plasmas in which Coulomb collisions are expected to predominate, an expression for plasma resistivity has been developed by Spitzer and Härm (ref. 6)

$$R = \frac{3.8 \times 10^5 Z \ln \Lambda}{T^{3/2}} \text{(ohm-meter)} \tag{32}$$

where Z is the ion charge in multiples of the electron charge and $\ln \Lambda$ is a function which is tabulated by Spitzer and Härm (ref. 6). The values of plasma conductivity calculated from equation (32) are shown in figure A-1, together with those values calculated from equation (30). It may be seen from this graph that for an argon plasma at a pressure of 1 cm Hg, the probe theory may be applied for temperatures up to the transition zone from "dilute" to dense which is 6,000°K to 8,500°K.

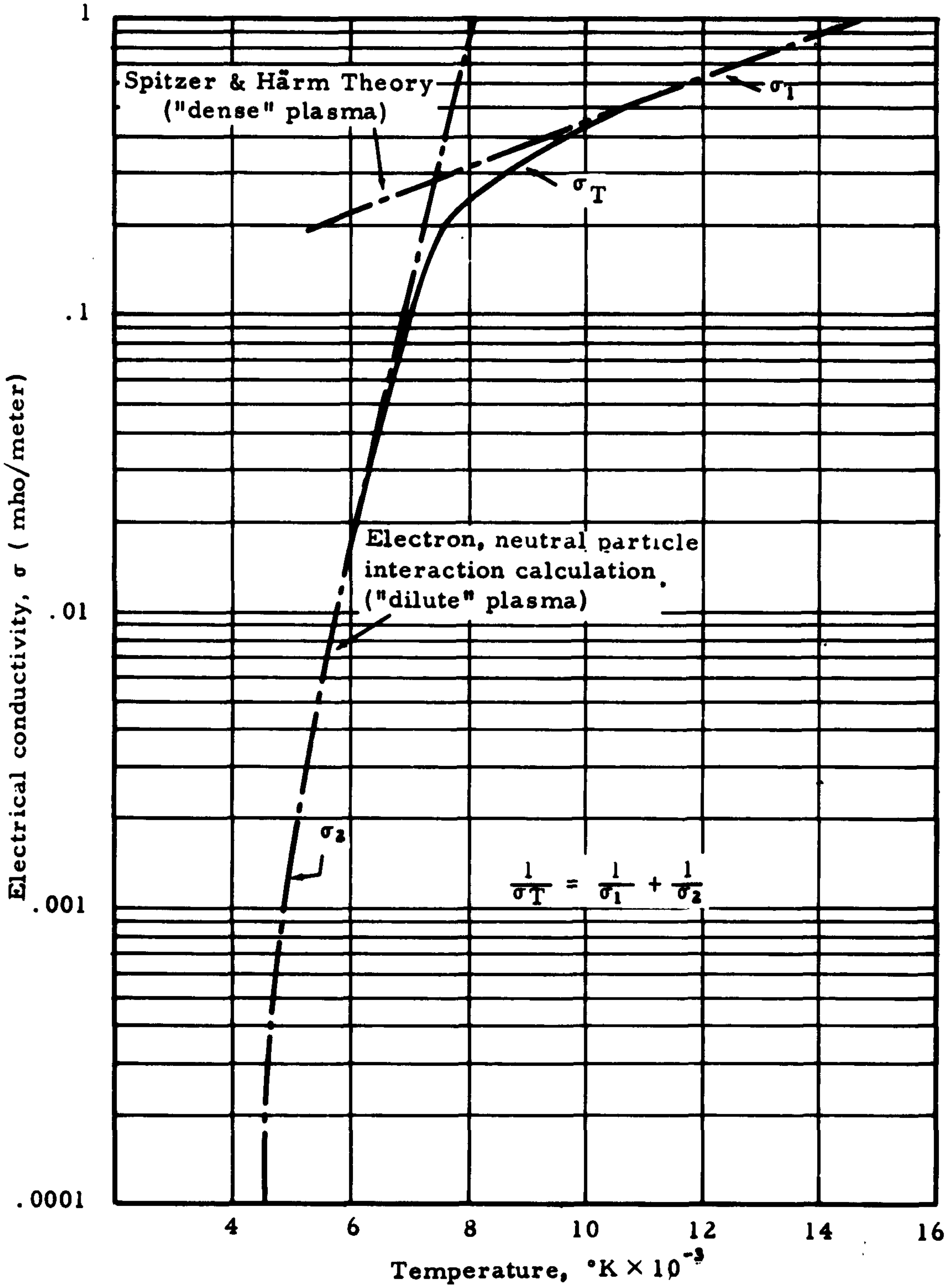

Figure A-1. - Electrical conductivity versus temperature for an argon plasma.

Appendix B

AN ANALYSIS OF SOME PROBE DATA BY THE GENERAL DOUBLE PROBE THEORY

Johnson and Malter (ref. 3) have obtained double probe data in quiescent decaying plasmas. Their data were obtained from plasmas generated by a pulse discharge. Probe currents versus time were measured at fixed values of potential difference between probes. The data shown in figure A-1 are taken directly from their paper. The points shown on the curve 1 were taken 400 sec after the plasma generating discharge had closed. This period was determined by Johnson and Malter to be sufficient to establish equilibrium. The area of each probe in their experiments was equal so that the ratio A_1/A_2 which appears in the simplified probe theory is unity for this discussion.

For A_1/A_2 less than a critical value which is determined by the ion mass in the plasma (see equation 20), the general probe theory gives the applied voltage-current relation by the equation

$$V_a = k/\epsilon T_{e_1} \ln(1 - I/i_{i_1}A_1) - k/\epsilon T_{e_2} \ln(1 + I/i_{i_2}A_2) + \Delta V_f \qquad (33)$$

where ΔV_f is the difference in plasma-probe potential between the two probes.

In order to use the data of Johnson and Malter in the above equation constant values of i_iA must be assumed. Observations of most data reveals the continued increase in I after the supposed saturation value of I has been reached. This increase in I is due to expansion of the sheath with voltage. The continued increase in I can be attributed to an effective increase of probe area, which occurs because of an increase in sheath volume produced by an increase in current to the probe. For a first approximation, this perturbation is assumed linear with I. The dashed lines on figure B-1 show how the magnitude of the perturbation has been estimated. The figure also shows the data of Johnson and Malter as modified by the perturbation correction. The modified data points were obtained by reducing the current I by an amount equal to the perturbation. For example, in figure B-1, the estimated perturbation on I at data point a is d' as shown by the solid bar between the dashed lines. Therefore, point a is lowered by an amount, d, and placed on the modified data chart of figure B-2. A similar correction was made for 17 other points.

The modified Johnson and Malter data were analyzed by the least squares method to fit the equation

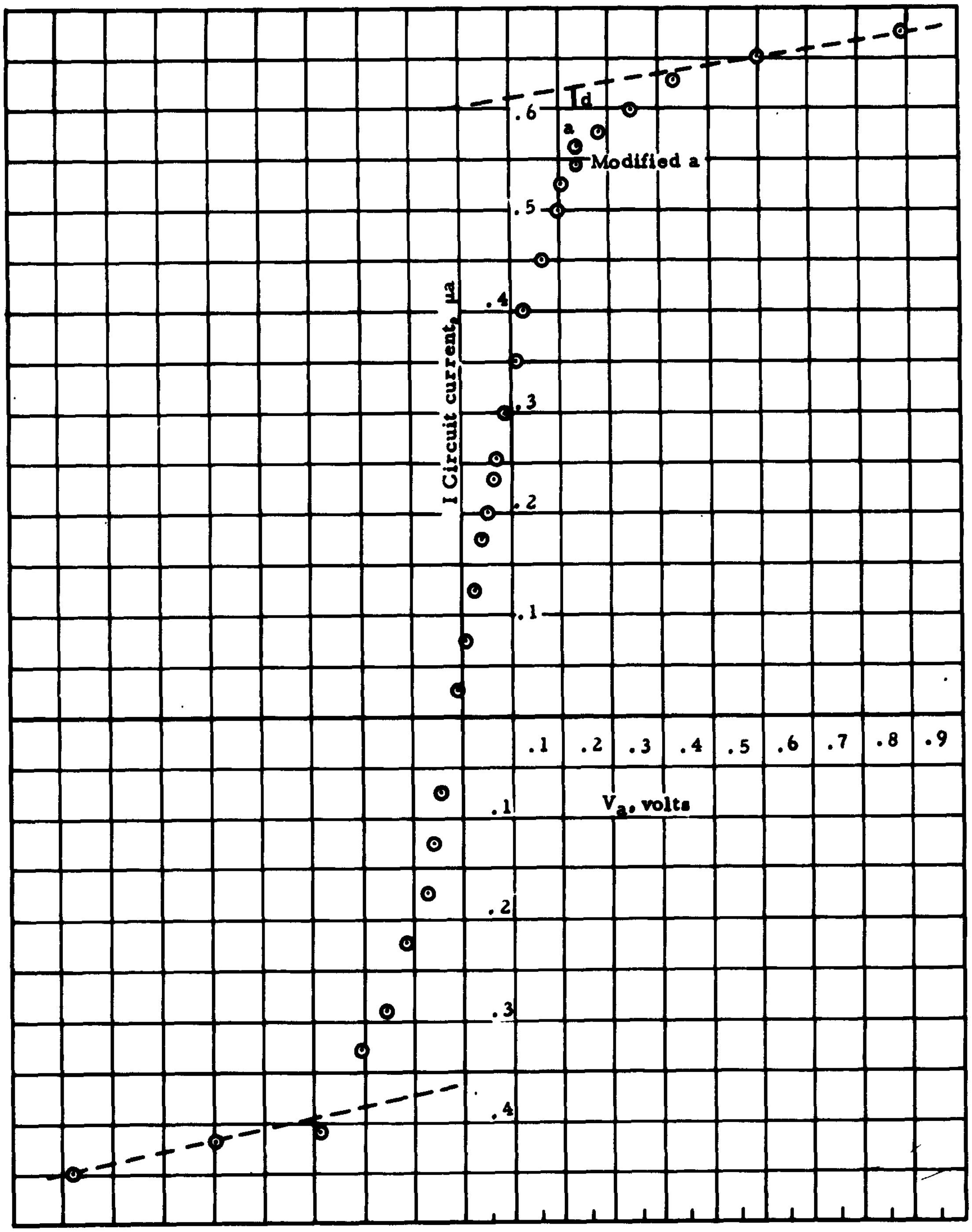

Figure B-1. - Double probe data from an argon plasma.

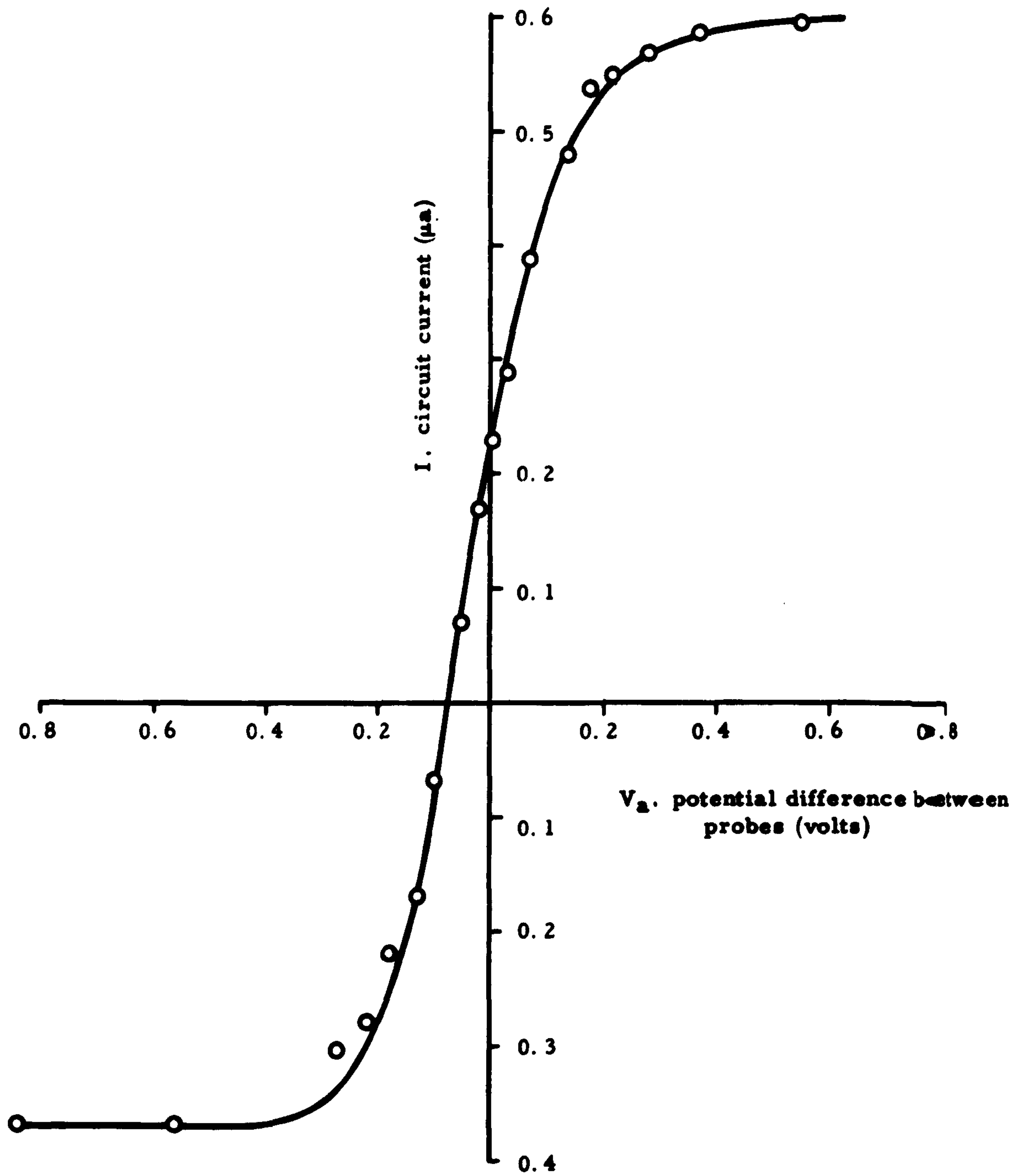

Figure B-2. - Eighteen corrected double probe data points and theory curve.

$$y_i = a_1 + a_2 \ln(1 - x_i/x_1) + a_3 \ln(1 + x_i/x_2) \tag{34}$$

which is of the same form as equation (32). The constants a_1, a_2, and a_3 are the unknowns to be determined. The x_i and y_i are the given data points. The values of x_1 and x_2 are determined graphically (see fig. B-2).

The equations which explicitly satisfy the least square minimization requirement for the problem cited here are:

$$O = \sum_m \left[a_1 + a_2 \ln(1 - x_i/x_1) + a_3 \ln(1 + x_i/x_2) - y_i\right] \tag{35}$$

$$O = \sum_m \left[a_1 + a_2 \ln(1 - x_i/x_i) + a_3 \ln(1 + x_i/x_2) - y_i\right] \ln(1 - x_i/x_1) \tag{36}$$

$$O = \sum_m \left[a_1 + a_2 \ln(1 - x_i/x_1) + a_3 \ln(1 + x_i/x_2) - y_i\right] \ln(1 + x_i/x_2) \tag{37}$$

Eighteen points were taken from the modified Johnson and Malter data. These points were chosen more or less uniformly along the current-voltage curve. The value of m in equations (35) through (37) therefore, runs from 1 through 18. It may be noted here that the present analysis does not fully utilize the data available, since there were 30 available data points. The values of the coefficients obtained from the simultaneous solution of equations (35) through (37) are: $a_1 = -0.07528$ volt, $a_2 = 0.07253$ volt, and $a_3 = -0.10045$ volt. The graphically determined values of x_1 and x_2 were used in equations (35) through (37); these values are: $x_1 = 0.3723$ amp and $x_2 = 0.6012$ amp. By comparing the coefficients a_1, a_2, and a_3 with their corresponding terms in equation (32), the electron temperatures at the probes and the difference in plasma-probe potentials were determined to be $T_{e_1} = 841°K$, $T_{e_2} = 1,165°K$, and $\Delta V_f = -0.07528$ volt. The curve in figure B-2 is generated from equation (34) after appropriate conversion of coefficients a_1, a_2, and a_3.

From the Langmuir theory as modified and used by Johnson and Malter, (ref. 3) the values of T_{e_1} and T_{e_2} are not obtained separately. However, they obtained an average value of T_e, the electron temperature, of $T_e = 1,015°K$. This value compares favorably with the arithmetic average of T_{e_1} and T_{e_2} which is 1,003°K.

<u>REFERENCES</u>

1. Druyvesten, M. J: The Low Voltage Arc. Zeitschrift f. Physik, vol. 64, 1930 p. 781.

2. Langmuir, I., and Mott-Smith, H. Jr.: Studies of Electrical Discharges in Gases at Low Pressures. General Electric Review, vol. 27, 1924, pp. 449, 538, 616, 762, 810.

3. Johnson, E. O., and Malter, L.: A Floating Probe Method for Measurements in Gas Discharges. Physical Review, vol. 80, 1950, p. 58.

4. Lin, S.: Electrical Conductivity of an Ionized Gas Produced by Strong Shock Waves. Doctorial Dissertation, Cornell University, 1952.

5. Quarterly Research Review No. 19, 1 August 1958 - 31 October 1958, Research Laboratory, ARGMA 2A19.

6. Spitzer, L.: Physics of Fully Ionized Gases. Interscience Publishers, Inc., New York, 1956.

DISTRIBUTION

	Copy
In accordance with Lists A and B of the Guided Missile Technical Information Distribution List, MML 200/23, List No. 23, 3 April 1961	1 - 192
Department of the Army Office, Chief of Ordnance Washington 25, D. C. ATTN: ORDTB	
Mr. E. L. Holoday	193
Mr. C. R. Cornthwaite	194
ORDTX	
Dr. R. B. Power, Jr.	195
Lt. Col. R. H. White	196
Commanding Officer Watertown Arsenal Watertown 72, Massachusetts ATTN: Ordnance Materials Research Office	197
Dr. J. L. Martin	198
Mr. J. A. Hofmann	199
Mr. Homer Priest	200
Laboratory	201
Mr. N. L. Reed	202
Mr. G. A. Darcy	203
Mr. P. Sagalyn	204
Commanding General Aberdeen Proving Ground Maryland ATTN: Ordnance Board	205
Lt. Col. K. E. Nelson	206
Dr. N. W. Arnold	207
Ballistic Research Laboratories	208
Lt. Col. G. Parsons	209
Dr. F. Kaufman	210
Commanding Officer U. S. Army Research Office (Durham) Box CM Duke Station Durham, North Carolina ATTN: Dr. J. W. Dawson	211
Dr. S. Githens	212-214
Mr. G. Cox	215
Chief Armed Forces Special Weapons Project Washington 25, D. C. ATTN: Document Library Branch	216
Department of the Army Chief of Research and Development Army Research Office Washington 25, D. C. ATTN: Capt. K. G. Comstock	217
Mr. Allan Tarr	218
Lt. Col. L. G. Klinker	219
Commanding Officer Watervliet Arsenal Watervliet, New York ATTN: Mr. P. M. Netzer	220
Dr. Fritz Sautter	221
Commanding Officer Ordnance Tank-Auto Command 1501 Beard Street Detroit 9, Michigan ATTN: Mr. S. H. Fuller	222
Mr. Fred Seppi	223
Mr. P. Hoffman-Pinther	224
Commanding General USA Ordnance Arsenal Frankford Philadelphia 37, Pennsylvania ATTN: Mr. W. J. Kroeger	225
Mr. M. Weinstock - 1421-5583	226
Dr. M. L. Chwalow	227
Commanding Officer Diamond Ordnance Fuze Laboratories Washington 25, D. C. ATTN: Mr. M. Apstein	228
Technical Reference Section	229
Commanding General Ordnance Weapons Command Rock Island, Illinois ATTN: Mr. W. G. Smith	230
Commanding Officer U. S. Army Signal Missile Support Agency White Sands Missile Range, New Mexico ATTN: SIGWS-EW	231
Commanding Officer Picatinny Arsenal Dover, New Jersey ATTN: Mr. S. Verner	232
Mr. W. R. Carson	233
Mr. S. Penn	234
ORDBB-THS	235
Liquid Rocket Propulsion Laboratory	236
Mr. S. Ritterman	237
Mr. A. Machenzie	238
Mr. W. Doremus	239
Mr. Menezes	240
Commanding General Detroit Arsenal 28251 Van Dyke Avenue Centerline, Michigan ATTN: ORDMX-B	241
Commanding Officer U. S. Army Signal Research and Development Laboratory Fort Monmouth, New Jersey ATTN: SIGFM/EL-P	242
SIGFM/EL-DP	243
SIGFM/EL-NA	244
SIGFM/EL-SA	245
Dr. S. B. Levin	246
Mr. Louis Reiss	247
Dr. H. Theissing	248
Director, Exploratory Res. Div. E	249
Director Waterways Experiment Station Vicksburg, Mississippi ATTN: Research Center Library	250
Office of the Director of Defense Research and Engineering Director of Weapons System Evaluation Group Room 2E812, The Pentagon Washington 25, D. C.	251-253
Quartermaster Research and Engineering Laboratories Natick, Massachusetts ATTN: Dr. J. M. Davies	254
Headquarters, Quartermaster Research and Development Command Natick, Massachusetts ATTN: Dr. G. R. Thomas	255
Mr. L. A. Spano	256
U. S. Army Engineering Research and Development Laboratory Fort Belvoir, Virginia ATTN: Mr. A. W. Van Heuckeroth	257
Mr. Harry Lowe	258
Dr. Wiseman	259

	Copy
U. S. Army Transportation Research and Engineering Command Fort Eustis, Virginia ATTN: Lt. V. DeFatta	260
Dr. G. D. Sands	261
Dr. J. S. diRende	262
U. S. Army Chemical Warfare Laboratories Army Chemical Center, Maryland ATTN: Mr. C. A. Butler	263
Mr. T. A. Treglia	264
Department of the Army Office, Chief of Engineers Directorate, Research and Development Building T-7 Washington 25, D. C. ATTN: Mr. E. F. Clark	265
Walter Reed Army Medical Center Prosthetics Research Laboratory Washington 25, D. C. ATTN: Dr. Fred Leonard	266
The Johns Hopkins University Operations Research Office 6935 Arlington Road Bethesda, Maryland ATTN: Dr. T. S. Needels	267
Dr. B. B. Watson	268
U. S. A. Medical Research and Development Command Dental Research Branch Main Navy Building Washington 25, D. C. ATTN: Lt. Col. P. M. Margetis	269
Commanding Officer U. S. Naval Propellant Plant Indian Head, Maryland	270
U. S. Naval Ammunition Depot Navy Number Six Six (66) c/o Fleet Post Office San Francisco, California ATTN: Ordnance Technical Library	271
Chief of Naval Research Department of the Navy Washington 25, D. C. ATTN: Code 426	272
Air Force Office of Scientific Research Temporary T Building 14th Street and Constitution Avenue, N. W. Washington 25, D. C. ATTN: SRP	273
SREC	274
Commander Wright Air Development Center Wright-Patterson Air Force Base, Ohio ATTN: WCLJD (Mr. E. Seebinger)	275
WCLTY (Mr. J. Wittebort)	276
WCLSE-11 (Capt. D. Harney)	277
Dr. Arthur E. Ruark Chief, Controlled Thermonuclear Branch Division of Research U. S. Atomic Energy Commission Washington 25, D. C.	278
Lewis Research Center National Aeronautics and Space Administration 21000 Brookpark Road Cleveland 35, Ohio ATTN: Mr. J. Sloop	279
Mr. C. E. Shepard	280
Exchange and Gift Division Library of Congress Washington 25, D. C.	281
Liquid Propellant Information Agency The Johns Hopkins University Applied Physics Laboratory 8621 Georgia Avenue Silver Springs, Maryland	282-284
Solid Propellant Information Agency The Johns Hopkins University Applied Physics Laboratory 8621 Georgia Avenue Silver Springs, Maryland	285
Central Intelligence Agency 2430 E Street, N. W. Washington 25, D. C. ATTN: OCR Standard Distribution	286-289
National Bureau of Standards Heat Division 207 West Building Washington 25, D. C. ATTN: Mr. C. M. Herzfeld	290
North American Aviation, Inc. 12214 Lakewood Boulevard Downey, California ATTN: Aerophysics Library	291
THRU Air Force Plant Representative WEAPO North American Aviation, Inc. Los Angeles International Airport Los Angeles 45, California	
CONVAIR Scientific Research Laboratory A Division of General Dynamics Corporation 5001 Kearney Villa Road San Diego 11, California ATT" Mr. A. L. Berlad	292
Bell Telephone Laboratories, Inc. Whippany, New Jersey ATTN: ARGMA Liaison Officer	293
Dr. Charles Hoover	294
Spectrolab, Inc. 7423 Varna Avenue N. Hollywood, California ATTN: Mr. A. E. Mann	295
Geophysics Corporation of America 700 Commonwealth Avenue Boston 15, Massachusetts ATTN: Mr. R. M. Chapman, Director of Engineering	296
Mr. Paul Dickerman Engineering Department Midway Laboratories 6238 S. Drexel Chicago, Illinois	297
Mr. J. Leith Potter, Manager Staff Engineering Gas Dynamics Facility ARO, Inc. Tullahoma, Tennessee	298
AVCO Research Laboratory 2385 Revere Beach Parkway Everett 49, Massachusetts ATTN: Librarian	299
AVCO Manufacturing Corporation Research and Advance Development Division 201 Lowell Street Wilmington, Massachusetts ATTN: Dr. R. R. John	300
Dr. Ralph Buhler Giannini Research Laboratory 18400 S. Main Street Santa Ana, California	301

DISTRIBUTION (Concluded)

	Copy
CONVAIR A Division of General Dynamics Corporation Mail Zone 6-172 San Diego 12, California ATTN: Mr. W. Short, Physics Section	302
Space Physics Research Group Room 235, Bldg. 152 Lawrence Radiation Laboratory P. O. Box 808 Livermore, California ATTN: Dr. C. D. Schrader	303
Advanced Development Laboratories Bendix Products Division Bendix Aviation Corporation South Bend 20, Indiana ATTN: Mr. A. O. Kresse	304
Dr. J. L. Martin	305
Dr. Abe M. Zarem Electro-Optical Systems 170 N. Daisy Avenue Pasadena, California	306
Dr. William Clohessy, Director Technical Development The Martin Company, Denver Division P. O. Box 179 Denver 1, Colorado	307
Mr. Frank Bradley, Director Requirements The Martin Company, Baltimore Division Baltimore 3, Maryland	308
Radio Corporation of America Moorestown, New Jersey ATTN: Mr. Alvin C. Gottlieb	309
Rocketdyne 6633 Canoga Avenue Canoga Park, California ATTN: Dr. Robert J. Thompson, Jr. Dr. C. J. McDole	310
Vidya 2626 Hanover Street Palo Alto, California ATTN: Dr. M. G. Boobar	311
Saint Louis University 221 N. Grand, St. Louis, Missouri ATTN: Mr. A. H. Weber, Physics Dept.	312
Project MATTERHORN James Forrestal Research Center Princeton University, P. O. Box 451 Princeton, New Jersey	313
Dr. C. W. Tombaugh Physical Science Laboratory New Mexico College of Agriculture and Mechanical Arts Box 548, State College, New Mexico	314
Professor Kurt Wohl Chemical Engineering Department University of Delaware Newark, Delaware	315
University of Alabama University, Alabama ATTN: Dr. F. H. Mitchell, Box 1392	316
Bureau of Engineering, Box 6162	317
Professor H. Kuenzel, Department of Mechanical Engineering	318
Department of Chemical Engineering	319
Dr. Loren E. Bollinger Rocket Research Laboratory Department of Aeronautical Engineering The Ohio State University Columbus 10, Ohio	320
Dr. Peter Debye Chemistry Department Cornell University Ithaca, New York	321

	Copy
Dr. Paul Gross Department of Chemistry Duke University Durham, North Carolina	322
Dr. J. Richard Haskins Gettysburg College Gettysburg, Pennsylvania	323
Dr. William D. Williams Harding College Box 602 Searcy, Arkansas	324
Prof. Paul W. Gilles Department of Chemistry The University of Kansas Lawrence, Kansas	325
Dr. Harold G. Donnelly, Head Chemical and Metallurgical Engineering Department Wayne State University Detroit 2, Michigan	326
Armour Research Foundation Illinois Institute of Technology Technical Center 10 W. 35th Street Chicago 16, Illinois	327
Rohm and Haas Company Redstone Arsenal Research Division Redstone Arsenal, Alabama ATTN: Librarian	328
Thiokol Chemical Corporation Redstone Division Redstone Arsenal, Alabama ATTN: Librarian	329
George C. Marshall Space Flight Center National Aeronautics and Space Administration Redstone Arsenal, Alabama ATTN: M-SAT-DIR (Dr. O. H. Lange)	330
M-S and M-M (Dr. W. R. Lucas)	331
M-RP-T (Mr. G. B. Heller, Mr. D. W. Gates)	332-341
National Aeronautics and Space Administration Manned Spacecraft Center Langley AFB, Virginia ATTN: Mr R. B. Erb	342
Mr. J. Kotanchik	343
Commanding General U. S. Army Ordnance Missile Command Redstone Arsenal, Alabama ATTN: ORDXM-XS	344
ORDXM-XE	345
ORDXM-XGR	346
ORDXM-R	347
ORDXM-RE	348
ORDXM-REX (Mr. E. T. Carr)	349
ORDXM-RF	350-354
ORDXM-RC	355
ORDXM-RP	356
ORDXM-RH	357
ORDXM-RI	358
ORDXM-RM	359-360
ORDXM-RK	361
ORDXM-RS	362
ORDXM-RG	363
ORDXM-RR	364-388
ORDXM-RB	389-391
ORDXM-RAP	392

AD ______________ Accession No. ______________

Army Rocket and Guided Missile Agency, Research and Development Operations, Research Laboratory, Redstone Arsenal, Alabama

A GENERAL PROBE THEORY FOR MEASUREMENTS IN A PLASMA (U) - Charles M. Cason and T. A. Barr, Jr.

ARGMA TR 2H4R, 1 Dec 61, 24 pp - illus.
Unclassified Report

The standard model of floating probes in plasmas is reviewed. It is shown that a maximum charge density exists for the application of this model. An explicit expression of voltage applied to the probes in terms of circuit current is obtained.

UNCLASSIFIED

1. Probe theories
2. Plasma - Temperature measurement
3. Plasma analysis
4. Probes, Langmuir
5. Probes, Johnson-Malter

I. Cason, Charles M.
II. Barr, T. A., Jr.

DISTRIBUTION: Copies obtainable from ASTIA, Arlington Hall Station, Arlington 12, Virginia.

AD ______________ Accession No. ______________

Army Rocket and Guided Missile Agency, Research and Development Operations, Research Laboratory, Redstone Arsenal, Alabama

A GENERAL PROBE THEORY FOR MEASUREMENTS IN A PLASMA (U) - Charles M. Cason and T. A. Barr, Jr.

ARGMA TR 2H4R, 1 Dec 61, 24 pp - illus.
Unclassified Report

The standard model of floating probes in plasmas is reviewed. It is shown that a maximum charge density exists for the application of this model. An explicit expression of voltage applied to the probes in terms of circuit current is obtained.

UNCLASSIFIED

1. Probe theories
2. Plasma - Temperature measurement
3. Plasma analysis
4. Probes, Langmuir
5. Probes, Johnson-Malter

I. Cason, Charles M.
II. Barr, T. A., Jr.

DISTRIBUTION: Copies obtainable from ASTIA, Arlington Hall Station, Arlington 12, Virginia.

AD ______________ Accession No. ______________

Army Rocket and Guided Missile Agency, Research and Development Operations, Research Laboratory, Redstone Arsenal, Alabama

A GENERAL PROBE THEORY FOR MEASUREMENTS IN A PLASMA (U) - Charles M. Cason and T. A. Barr, Jr.

ARGMA TR 2H4R, 1 Dec 61, 24 pp - illus.
Unclassified Report

The standard model of floating probes in plasmas is reviewed. It is shown that a maximum charge density exists for the application of this model. An explicit expression of voltage applied to the probes in terms of circuit current is obtained.

UNCLASSIFIED

1. Probe theories
2. Plasma - Temperature measurement
3. Plasma analysis
4. Probes, Langmuir
5. Probes, Johnson-Malter

I. Cason, Charles M.
II. Barr, T. A., Jr.

DISTRIBUTION: Copies obtainable from ASTIA, Arlington Hall Station, Arlington 12, Virginia.

AD ______________ Accession No. ______________

Army Rocket and Guided Missile Agency, Research and Development Operations, Research Laboratory, Redstone Arsenal, Alabama

A GENERAL PROBE THEORY FOR MEASUREMENTS IN A PLASMA (U) - Charles M. Cason and T. A. Barr, Jr.

ARGMA TR 2H4R, 1 Dec 61, 24 pp - illus.
Unclassified Report

The standard model of floating probes in plasmas is reviewed. It is shown that a maximum charge density exists for the application of this model. An explicit expression of voltage applied to the probes in terms of circuit current is obtained.

UNCLASSIFIED

1. Probe theories
2. Plasma - Temperature measurement
3. Plasma analysis
4. Probes, Langmuir
5. Probes, Johnson-Malter

I. Cason, Charles M.
II. Barr, T. A., Jr.

DISTRIBUTION: Copies obtainable from ASTIA, Arlington Hall Station, Arlington 12, Virginia.